International Journal for Multidisciplinary Research (IJFMR)
E-ISSN: 2582-2160 ● Website: www.ijfmr.com ● Email: editor@ijfmr.com

A Computational Insight Into The Reactivity, Aromaticity, And Absorption Spectra Of Six Membered Isoelectronic N-Heteroarenes

Bapan Saha

Corresponding author: Department of Chemistry, Handique Girls' College, Guwahati-781001

Abstract:
Reactivity, aromaticity, and absorption spectra of pyridine, pyridazine, pyrimidine, pyrazine, 1,2,3-triazine, 1,2,4-triazine and 1,2,5-triazine are studied in the light of Density functional theory (DFT) at B3LYP/6-31+G(d,p) level of theory. Frontier molecular orbitals are studied, both HOMO and LUMO energies and their shapes changes on increasing the number of N-atom in the rings. Global hardness (η) and global electrophilicity (ω) values comply with both MHP and MEP. In plane and out of plane aromaticity vary significantly with change in the position and number of N-atom in the ring, and maximum aromaticity is found around 1.0 Å from the molecular plane. Time dependent density functional theory (TDDFT) is study has suggested their absorption maxima primarily in the UV-region, and shows both red and blue shift depending upon the position and number of N-atom in the heteroarenes.

Keywords: HOMO-LUMO gap, global hardness, electrophilicity, aromaticity, TD-DFT, absorption spectra

1. Introduction

N-heteroarenes contains a ring structure with one or more N-atoms. They are aromatic in nature and exhibit unique electronic properties. These heteroarenes have profound application in the field of catalysis, material science, pharmaceutical, environmental domain.[1-4] Apart from these, N-heteroarenes have also been used in functionalizing carbon nanomaterials thereby enhancing their surface activity.[1-4] N-heteroarenes play significant roles in the chemical processes both in plant and animal. Substances such as chlorophyll of plants and heme unit of blood, components of nucleic acids, coenzymes, amino acids, alkaloids etc. also contain N-heteroarenes are one of the components.[1-4] N-heteroarenes (especially five and six membered), like other aromatic compounds, contain a closed system of $(4n + 2)$ π-electrons and their chemistry is determined by the specific nature of each heterocyclic ring.[5,6]

Experimental studies on some properties of 6-membered N-heteroarenes have previously been reported.[7,8] From the view point of their utility and applicability, a systematic understanding about different properties of N-heteroarenes imperative. Density functional theory (DFT) provides useful information about energetic, structure and properties of molecules at much lower costs than wave function technique[9] and has been widely used in studying different properties of molecular systems. Therefore, an attempt has been made to study the global reactivity descriptors viz. global hardness, chemical potential and philicity, and local reactivity descriptors such as Fukui function, electrophilicity index of a few six membered isoelectronic N-heteroarenes viz. pyridine, pyridazine, pyrimidine, pyrazine, 1,2,3-triazine, 1,2,4-triazine

and 1,2,5-triazine using DFT. Variation in dipole moments is also scrutinized. Apart from this, energy, and shape of frontier molecular orbitals (FMOs), in plane and out of plane aromaticity and UV-Visible absorption (gas and solvent phase) spectra of these N-heteroarenes are also studied.

2. Theoretical and computational details:

Chemical potential (μ) and global hardness (η) are defined as the first and second derivative of energy with respect to the number of electrons respectively.[10] Use of finite difference approximation and Koopmans' theorem[11] lead to the working formulae for μ and η as: $\eta = (E_{LUMO}–E_{HOMO})/2$, $\mu = (E_{LUMO} + E_{HOMO})/2$. Parr and co-workers proposed electrophilicity (ω) as a measure of electrophilic power of a ligand and its propensity to soak up electrons[12] and mathematically $\omega = \mu^2/2\eta$. Herein, E_{LUMO} is the energy of lowest unoccupied molecular orbital (LUMO) and E_{HOMO} is the energy of the highest occupied molecular orbital (HOMO).

All calculations are carried out using Gaussian 09 program.[13] The geometrical minima of the species are obtained using Becke three parameter exchange and Lee, Yang and Parr correlation functional (B3LYP) in combination with 6-31+G(d,p) basis set. The geometrical minima are ensured by presence of real frequency in the frequency calculation. Reactivity parameters are calculated by using the abovesaid equations. Aromaticity of the chosen N-heteroarenes by estimating the nucleus independent chemical shift (NICS) values.[14] Gauze Independent Atomic Orbital (GIAO) method is used to calculate the aromaticity by placing a Bq atom at the centre of the molecular plane and out of the plane.[14] Throughout the manuscript, negative value of isotropic shift is reported. Solvent phase analysis of the aforesaid parameters is also scrutinized. TD-DFT (time dependent density functional theory) is used for studying the UV-Visible absorption spectra of a system.[15] Absorption spectra of the concerned system are interpreted using N=10 method at the same level of theory. Solvent phase analysis of UV-Visible absorption spectra is studied in two model solvents viz. cyclohexane and DMSO using Polarizable Continuum Model (PCM).[16]

3. Results and discussions:

3.1 Molecular Electrostatic Potential Surface:

The reactivity at a particular site can be predicted by considering the concept of molecular electrostatic potential MEP).[17] Therefore, MEP surface for the chosen N-heteroarenes is studied along with calculation of $V_{s(max)}$ (region of electron deficient region) and $V_{s(min)}$ (region of electron excess region) values and the obtained results are presented in **Figure 1**. The appearance of yellow-red color in the MEP surface indicates the region with high electron density while presence of blue color in the same indicates the region associated electron deficiency.[17] Referring to **Figure 1**, it is seen that, the region around N-atom is reddish in color, thereby indicating the high electron density around the heteroatom. This is also expected, and is attributed to the higher electronegativity of N-atom compared to C-atom. Rest of the part of the heteroarenes are greenish or bluish in color, thus indicating electron deficient region. $V_{s(max)}$ around the H-atom of the N-heteroarenes are found to be within the range from 20.84 to 34.91 kcalmol^{-1} and $V_{s(min)}$ around the N-atom of the N-heteroarenes are found to be within the range from -25.77 to -41.80 kcalmol^{-1}, **Figure 1**. Thus, area around N-atom will be prone to electrophilic attack while other region is expected to susceptible to nucleophilic attack. Thus, presence of N-atom at different positions brings about unsymmetrical charge distribution at the region around N-atom in the heterocyclic ring and govern the local reactivity and site selectivity to some extent.

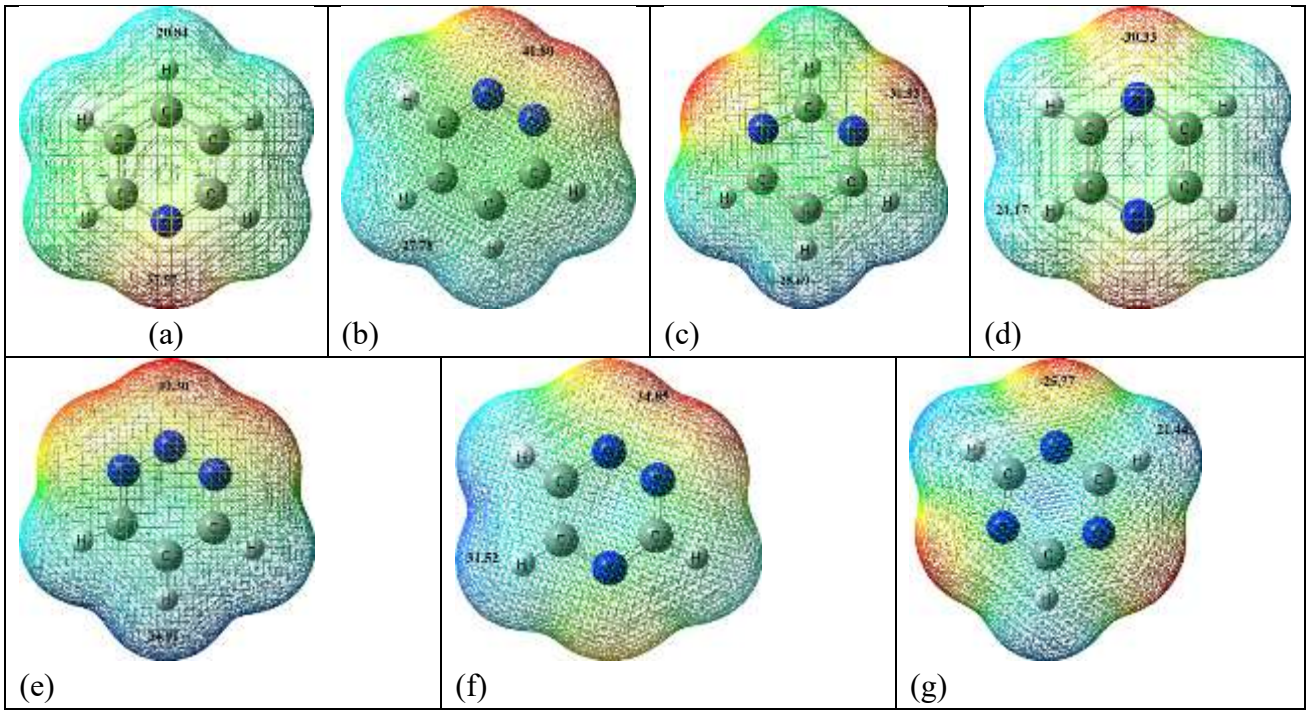

Figure 1 MEP surfaces along with $V_{s(max)}$ and $V_{s(min)}$ for (a) pyridine, (b) pyridazine, (c) pyrimidine, (d) pyrazine, (e) 1,2,3-triazine, (f) 1,2,4-triazine and (g) 1,2,5-triazine

3.2 Geometry of the optimized structures

The optimized structures of the concerned systems at B3LYP/6-31+G(d,p) level of theory are given in **Figure 2**. From the figure, it is obvious that presence of heteroatoms in the ring brings about some kind of distortions in the ring. This can be attributed to size difference between C and N-atoms. However, planarity of all the chosen N-heteroarene remains intact.[18] The C-C, C-N and N-N bond lengths are found to be within the range 1.39-1.41Å, 1.33-1.34 Å and 1.32-1.34 Å respectively.

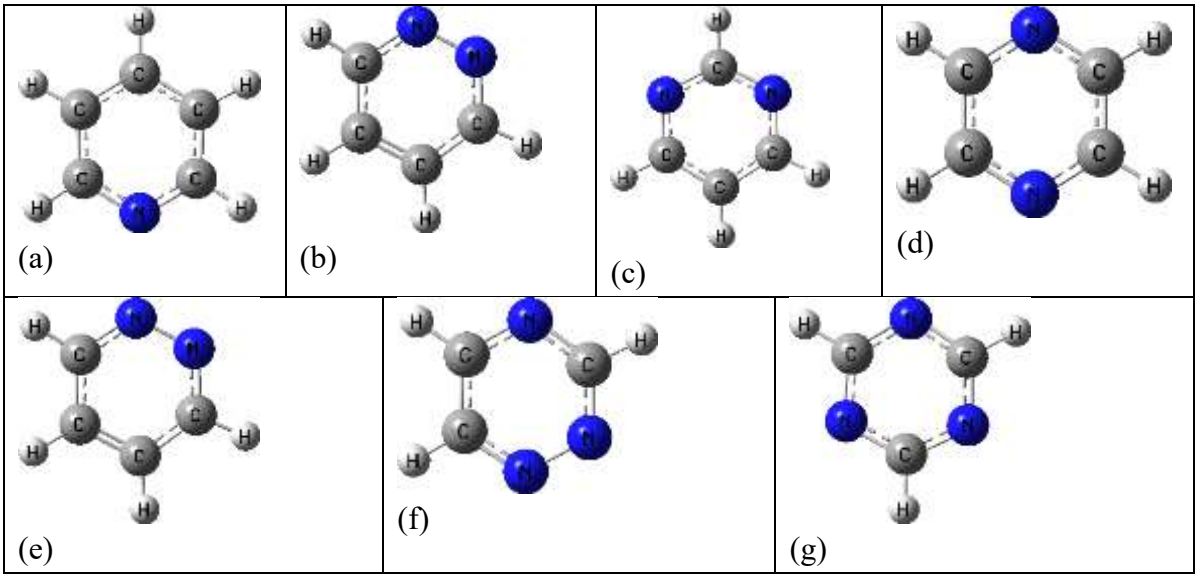

Figure 2 The optimized geometries of (a) pyridine, (b) pyridazine, (c) pyrimidine, (d) pyrazine, (e) 1,2,3-triazine, (f) 1,2,4-triazine and (g) 1,2,5-triazine

3.3 Variation in shapes and energy of HOMO and LUMO, and Dipole moment

Shapes of HOMO and LUMO is important in describing the electron donor and acceptor sites in a system[18] and therefore, their shapes are studied and depicted in **Figure 3**. Referring to the figure, HOMO of the chosen N-heteroarenes is primarily located near the N-atom present in the ring and LUMO is located on the area further from the N-atom residing on the chosen rings. Thus, electron donating capacity of these heteroarenes is predominantly associated with the N-atom present on the ring system while the electron accepting capacity of the molecules are associated with the C-atoms present in the ring system.[18] This is also expected, because N-atom in all these heteroarenes possess lone pair of electrons and is available for donation to suitable acceptors.

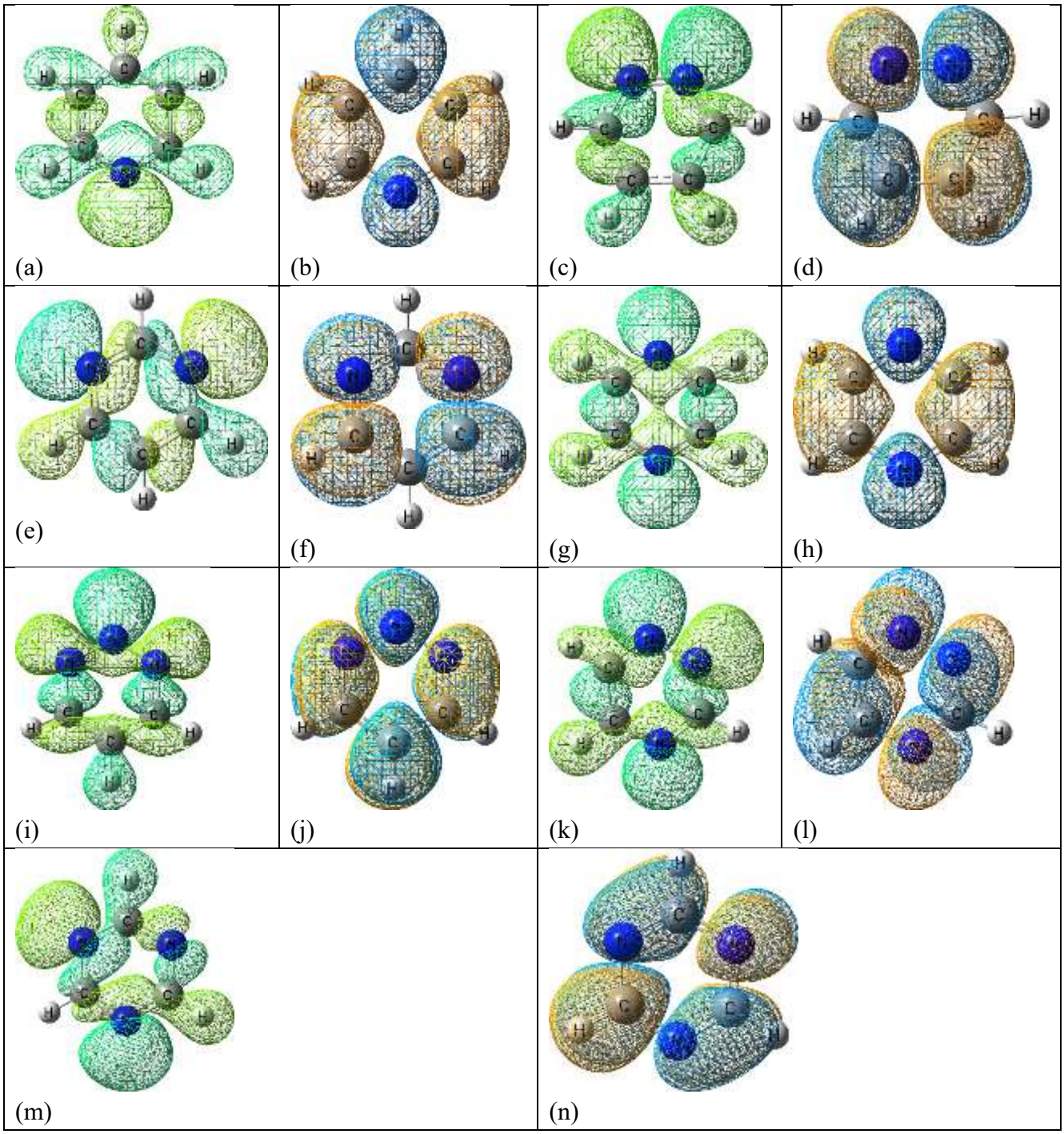

Figure 3: Shapes of FMMOs (a) HOMO of pyridine, (b) LUMO of pyridine (c) HOMO of pyridazine, (d) LUMO of pyridazine (e) HOMO of pyrimidine, (f) LUMO of pyrimidine (g)

HOMO of pyrazine, (h) LUMO of pyrazine (i) HOMO of 1,2,3-triazine, (j) LUMO of 1,2,3-triazine (k) HOMO of 1,2,4-triazine, (l) LUMO of 1,2,4-triazine, (m) HOMO of 1,2,5-triazine, (n) LUMO of 1,2,5-triazine

Measurement of E_{HOMO} of a species happens to be an important factor because of two reasons. Firstly, it measures the electron donating ability i.e., the reactivity of the species and secondly it governs the absorption spectra of the molecule (along with E_{LUMO}).[18] The E_{HOMO}, E_{LUMO}, HOMO-LUMO gap (ΔE), IE and EA obtained at B3LYP/6-31G+(d,p) level of theory in gas phase (in kcal/mol) is presented in **Table 1**. Since, the chosen species are isoelectronic, their stability can be predicted from their E_{HOMO} values. More negative (lower) the E_{HOMO}, higher is the stability of the systems. E_{HOMO} values for the chosen N-heteroarenes are found to be -165.96, -154.55, -167.33, -167.87, -169.23, -161.41 and -182.68 kcalmol^{-1} for pyridine, pyridazine, pyrimidine, pyrazine, 1,2,3-Triazine, 1,2,4-Triazine and 1,3,5-Triazine respectively. If more negative E_{HOMO} is used as measure of stability, 1,3,5-Triazine is the most stable six membered N-heteroarenes while pyridazine is the less stable isoelectronic species. Thus, presence and position of N-atom in the ring modulates the electron donating ability and thereby reactivity of the chosen systems. The observed E_{LUMO} values for the chosen systems are found to be within the range -24.89 to -58.75 kcalmol^{-1}. Thus, the chosen systems are prone to release its electrons for reaction quite readily. In HOMO-LUMO gap (ΔE) values not only measures the stability but also give key information about the band gap of chosen systems.[18] It predicts whether a substance a conductor, semiconductor, or insulator. For a system with large band gap (> 95 kcalmol^{-1}) are said to be insulator while a considerably small band gap, the system is known to be conductor while any intermediate value corresponds to semiconducting properties. It is seen that ΔE values are all >100 kcal mol^{-1}, thereby indicating their insulating nature. Large the band gap, larger is the stability. Thus, 1,3,5-triazine is the most stable while 1,2,4-triazine is the least stable. Frontier molecular orbitals are almost unaffected in presence of solvent phase.

Table 2 HOMO and LUMO energies, and band gap (HOMO-LUMO gap), Dipole moment (D) for the systems in kcalmol^{-1}

Systems	E_{HOMO}	E_{LUMO}	ΔE	Dipole moment
Pyridine	-165.96	-24.89	-141.07	2.38
Pyridazine	-154.55	-41.77	-112.78	4.42
Pyrimidine	-167.33	-36.50	-130.83	2.48
Pyrazine	-164.87	-42.37	-122.51	0.0
1,2,3-triazine	-169.23	-53.95	-115.27	5.24
1,2,4-triazine	-161.41	-58.75	-102.66	2.74
1,3,5-triazine	-182.68	-45.43	-137.25	0.0

Polarity of a system provides useful information about the solubility of a system along with its propensity to behave in solvent systems. Therefore, dipole moments for the chosen systems are studied and the calculated dipole moments are given in **Table 2**. It is seen that, dipole moment for the system varies significantly depending (from 0.0 to 5.24 D) on the number and position of N-atom in the ring. Pyrazine and 1,3,5-triazine are non-polar and hence expected to be soluble in non-polar solvents. On the other hand, polarity of the other N-heterocycles increased in the order: Pyridine (2.38 D) < Pyrimidine (2.48 D) < 1,2,4-triazine (2.74 D) < Pyridazine (4.42 D) < 1,2,3-triazine (5.24 D). Presence of solvent phase exerts nominal impact on the dipole moment of the chosen systems.

3.4 Global Reactivity descriptors:

Chemical stability of a system can be predicted from the variation of relativity parameters, viz global hardness (η), chemical potential (μ) and electrophilicity (ω).[18] The variation of global hardness, chemical potential and electrophilicity are studied and the gas phase results are presented in **Table 3**. From the table global reactivity descriptors viz. η, μ and ω change with variation in the position and number of N-atom present in the heteroarenes.[18] This may be attributed to the change in electron density produced due to the presence of heteroatoms in different positions. η value decreased in the order: Pyridine (70.53) > 1,3,5-triazine (68.62) > Pyrimidine (65.41) > Pyrazine (61.24) > 1,2,3-triazine (57.64) > Pyridazine (56.39) > 1,2,4-triazine (51.33); values are in kcalmol^{-1}. Higher the η value, higher is the stability. Thus, pyridine is expected to be most stable and 1,2,4-triazine is expected to be least stable amongst all. With few exceptions, μ and ω values also predicted similar stability of the chosen N-heteroarenes.

Table 3: Variation in global hardness (η), chemical potential (μ) and philicity (ω) in kcal/mol

Systems	η	μ	ω
Pyridine	70.53	-95.42	64.55
Pyridazine	56.39	-98.16	85.43
Pyrimidine	65.41	-101.91	79.38
Pyrazine	61.24	-103.61	87.63
1,2,3-triazine	57.64	-111.59	108.02
1,2,4-triazine	51.33	-110.08	118.03
1,3,5-triazine	68.62	-114.05	94.77

The comparative variation between electronic energy and global hardness and, global hardness and electrophilicity is shown in **Figure 4**. Although, global hardness is a measure of chemical stability of a molecular system, there is found to be no strong correlation (R^2 =0.26) between electronic energy and global hardness (**Figure 4a**). In other words, a system with highest global hardness does not possess least electronic energy in all the cases. From **Figure 4b**, it is obvious that MHP (Maximum Hardness Principle-higher the hardness higher is the stability) and MEP (Minimum Electrophilicity Principle-lower the philicity higher is the stability) principles is valid for most of the chosen N-heteroarenes.[18] By applying these two principles we can infer that pyridine has maximum stability (less reactive) and 1,2,4-triazine has minimum stability (more reactive) amongst the considered systems. NO considerable variation in reactivity parameters is observed in presence of solvent phase.

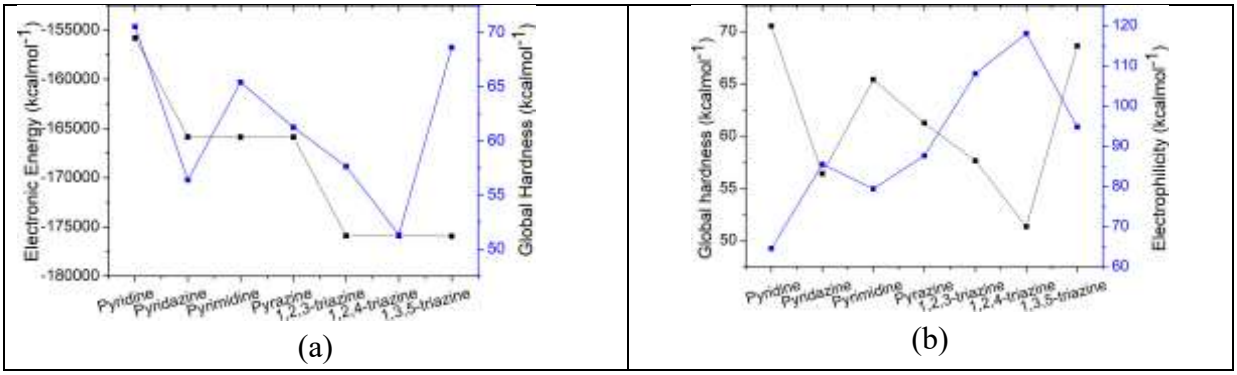

(a) (b)

Figure 4 Variation between (a) electronic energy and global hardness and (b) global hardness and philicity

3.5 Aromaticity:

Aromaticity cannot be measured directly, can be quantified by measuring structural, energetic, magnetic and electronic properties that are associated with aromatic compounds.[19-21] Magnetic properties of a species depends directly on the induced ring current and is an useful tool to gauge aromatic properties.[19-21] NICS is one of the most extensively used protocols to estimate aromaticity and can have positive (anti-aromatic) and negative (aromatic) values.[19-21] A non-aromatic system possesses NICS value close to zero.[19-21] $NICS_{iso}$ and $NICS_{zz}$ values can be used to predict aromatic character of a ring system. Since $NICS_{zz}$ values provides more accurate information about the π-electrons hence $NICS_{zz}$ values are calculated for the chosen N-heteroarenes.[18-21] In addition to in plane $NICS_{zz}$ (0) value, $NICS_{zz}$ (0.25), $NICS_{zz}$ (0.50), $NICS_{zz}$ (0.75) upto $NICS_{zz}$ (2.00) values are also computed over these distances from the centre of the plane of the ring (these values are scanned).

Table 4: $NICS_{zz}$ values of the chosen systems at varying distances.

Systems	Pyridine	Pyridazine	Pyrimidine	Pyrazine	1,2,3-triazine	1,2,4-triazine	1,3,5-triazine
$NICS_{zz}$ (0)	-12.62	-11.06	-10.18	-12.01	-9.65	-9.45	-6.91
$NICS_{zz}$ (0.25)	-21.80	-14.32	-13.35	-15.12	-13.28	-12.93	-10.36
$NICS_{zz}$ (0.50)	-26.80	-21.14	-20.09	-21.68	-20.68	-20.10	-17.65
$NICS_{zz}$ (0.75)	-28.29	-26.47	-25.42	-26.78	-26.25	-25.62	-23.42
$NICS_{zz}$ (1.00)	-26.70	-27.95	-27.01	-28.11	-27.64	-27.07	-25.27
$NICS_{zz}$ (1.25)	-23.48	-26.25	-25.44	-26.31	-25.73	-25.28	-23.86
$NICS_{zz}$ (1.50)	-19.83	-22.92	-22.27	-22.92	-22.30	-21.94	-20.83
$NICS_{zz}$ (1.75)	-16.38	-19.24	-18.69	-19.19	-15.13	-18.28	-17.42
$NICS_{zz}$ (2.00)	-15.15	-15.79	-15.36	-15.74	-12.65	-14.92	-14.25

The variation of $NICS_{(zz)}$ values with distance from the Bq atom for the concerned system of the heterocyclic ring are depicted in **Figure 5**. Referring to **Table 4** and **Figure 5**, it is apparent that the molecular plane of the chosen systems is aromatic with NICSzz values within the range -9.45 to -12.62. The molecular plane of Pyridine is most aromatic while 1,2,4-triazine is the least aromatic. Moreover, $NICS_{(zz)}$ values are distant dependent. With increase in the distance from the molecular plane the $NICS_{(zz)}$ values become more negative around ~1.0 Å from the molecular plane. On moving further from the molecular plane, the $NICS_{(zz)}$ values become less negative, **Table 4** and **Figure 5.** The diatropic ring current predominates around ~1.0 Å from the molecular plane thereby increasing the aromaticity. With increase in distance further, the diatropic ring current decreases resulting in decrease in aromaticity.[18-21] Recent literature has also indicated similar observation for N-doped graphene.[18] Thus, it can be inferred that presence of N-atom in the heterocycle at different positions alters the ring current induced which controls their aromaticity and hence reactivity of the heterocycles. In presence of solvent phase, no variation in aromaticity is observed.

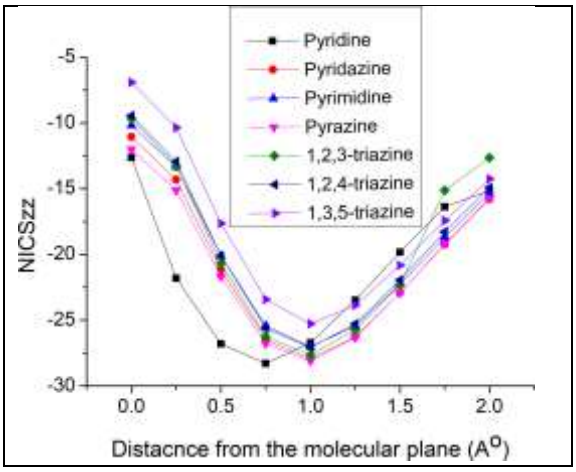

Figure 5: Variations in NICS$_{(zz)}$ values with the distances of from the plane

3.6. UV-Visible Spectra:

When a molecule absorbs some radiation, it goes to excited state. However, at excited state the molecule is reluctant to exists and it releases radiation and comes back to the ground state. The wavelength of the emitted radiation gives characteristic bands.[22] UV-Visible absorption spectra of the chosen compounds are studied at the same level of theory (B3LYP/6-31G(d,p)) in gas and solvent phase (cyclohexane and DMSO) and the observed results are depicted in **Figure 6**. The corresponding wavelength, excitation energy, predominant orbital involved in the transition for the chosen N-heteroarenes in are shown in **Table 5 (**gas phase**)**, **Table 6 (**cyclohexane**)**, **Table 7 (**DMSO**)**.

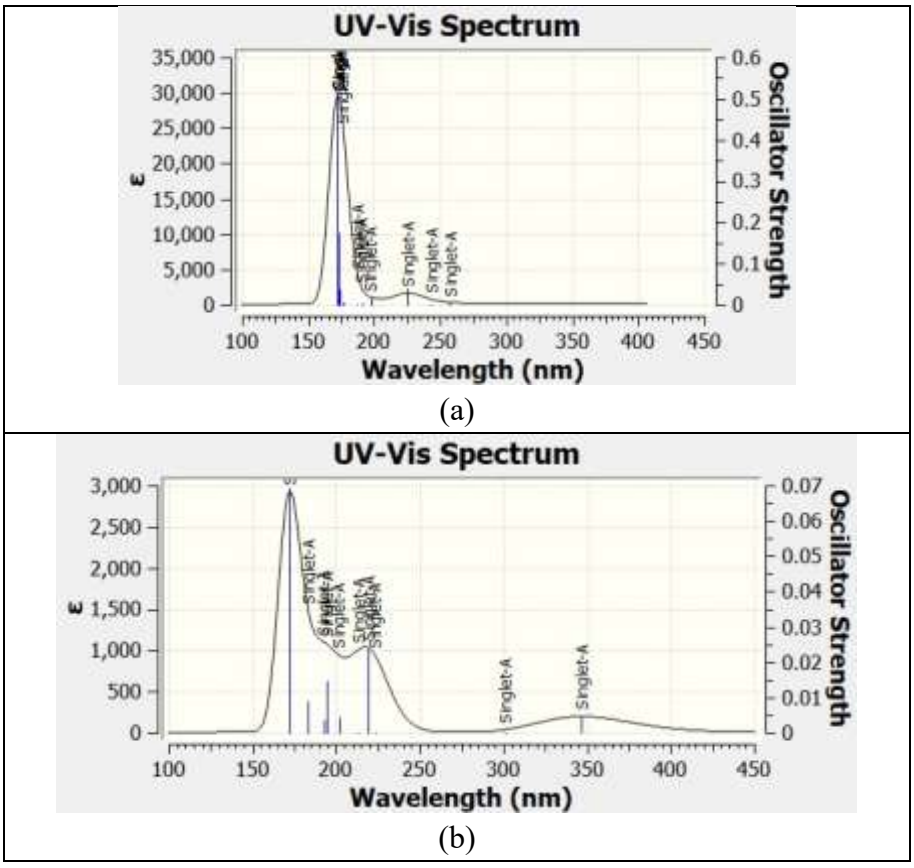

(a)

(b)

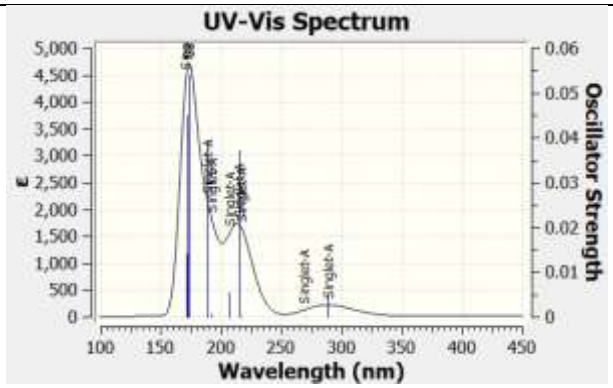
UV-Vis Spectrum
ε
Oscillator Strength
Wavelength (nm)
Singlet-A

(c)

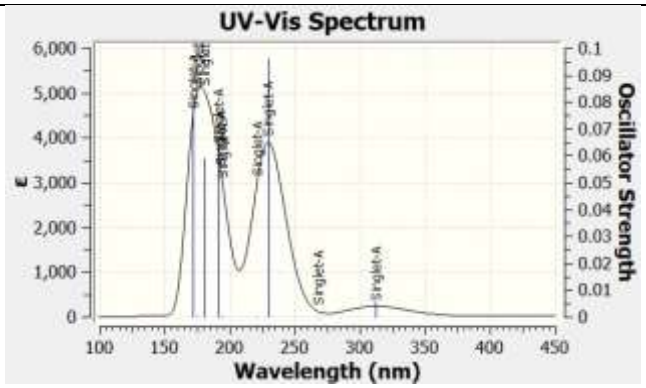
UV-Vis Spectrum
ε
Oscillator Strength
Wavelength (nm)
Singlet-A

(d)

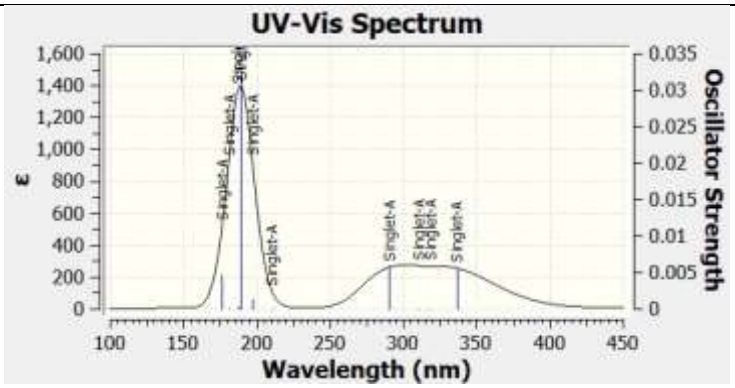
UV-Vis Spectrum
ε
Oscillator Strength
Wavelength (nm)
Singlet-A

(e)

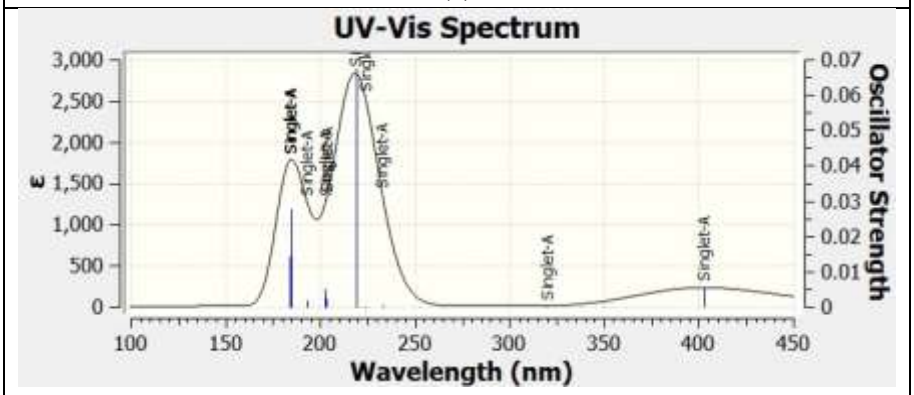
UV-Vis Spectrum
ε
Oscillator Strength
Wavelength (nm)
Singlet-A

(f)

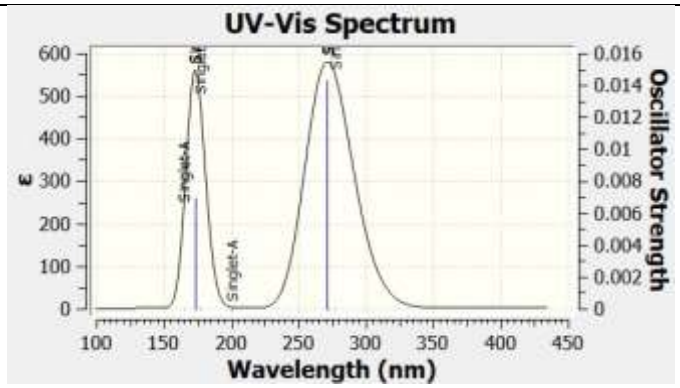

(g)

Figure 6: Absorption spectra (a) pyridine, (b) pyridazine, (c) Pyrimidine, (d) pyrazine, (e) 1,2,3-triazine, (f) 1,2,4-triazine and (g) 1,3,5-triazine in gas phase

Table 5. Excitation energies, corresponding wavelength, predominant transitions, and orbital contribution in gas phase

Systems	λ_{max}	f (oscillator frequency)	Orbital contribution	FMO	Energy (eV)
Pyridine	172.2 225.6	0.51 0.04	0.56 0.61	HOMO-2→LUMO+1 HOMO-1→LUMO	7.20 5.49
Pyridazine	172.0 219.4	0.07 0.03	0.64 0.59	HOMO→LUMO+5 HOMO-1→LUMO	7.21 5.65
Pyrimidine	174.2 215.4	0.05 0.03	0.69 0.60	HOMO→LUMO+3 HOMO-1→LUMO	7.13 5.70
Pyrazine	180.7 229.7	0.06 0.09	0.70 0.66	HOMO-1→LUMO+3 HOMO-1→LUMO	6.86 5.40
1,2,3-triazine	189.4 290.5 336.8	0.03 0.01 0.01	0.59 0.70 0.70	HOMO-2→LUMO HOMO-1→LUMO HOMO→LUMO	6.54 4.26 3.68
1,2,4-triazine	184.5 219.0 403.0	0.03 0.07 0.01	0.67 0.64 0.71	HOMO→LUMO+3 HOMO-1→LUMO HOMO→LUMO	6.72 5.66 3.07
1,3,5-triazine	173.3 271.5	0.07 0.01	0.70 0.51	HOMO→LUMO+2 HOMO→LUMO+1	7.15 4.57

In the gas phase, pyridine shows absorption maxima at 172.2 nm (narrow, high intensity) and 225.6 nm (broad, low intensity), **Figure 6** and **Table 5**. Experimental studies on pyridine show absorption maxima at 204 nm and 256 nm.[23] The observed results are close to the experimental results thereby validating the use of B3LYP/6-31+G(d,p) level of theory for studying the UV-Visible absorption spectra of the chosen N-heterocycles. The observed absorption maxima for pyridine can be attributed to the n→ π^* and $\pi\rightarrow\pi^*$ transitions (HOMO-2→LUMO+1 and HOMO-1→LUMO transition), **Figure 6a** and **Table 5**. Comparing the λ_{max} value of pyridine, it is seen that λ_{max} values for the high intensity maxima is almost unshifted for pyridazine and pyrimidine, **Figure 6a** and **Table 5**. However, in case of pyrazine red shift is observed with λ_{max} value of 180.7 nm (attributed to HOMO-1→LUMO+3 transition). Previous literatures have also

indicated the absorption spectra within similar range of maxim.[23,24] In case of 1,2,3-triazine, three absorption maxima are observed viz. at 189.4 (narrow and high intensity, HOMO-2→LUMO transition), 290.5 (HOMO-1→LUMO transition) and 336.8 nm (HOMO→LUMO transition). Similarly for 1,2,4-triazine three absorption maxima are observed: 184.5 (HOMO→LUMO+3 transition), 219.0 (HOMO-1→LUMO transition) and 403.0 nm (HOMO→LUMO transition). Although three maxima are observed in both the cases, the observed maxima are both blue and red shifted. However, in case of 1,3,5-triazine, two absorption maxima at 173.3 (HOMO→LUMO+2 transition) and 271.5 nm (HOMO→LUMO+1 transition) are observed. Thus, position of N-atom plays key role in controlling the absorption spectra of the chosen molecules, especially of triazines.

In presence of solvent phase (cyclohexane and DMSO), similar results are mostly obtained (cyclohexane and DMSO) with slight shifts in their absorption maxima, **Figure 7** and **8**, and **Table 6** and **7**. In solvent phase, absorption maxima are red shifted by ~4-5 nm in most cases. Thus, presence of solvent phase exerts nominal impact on the absorption spectra of the chosen N-heteroarenes

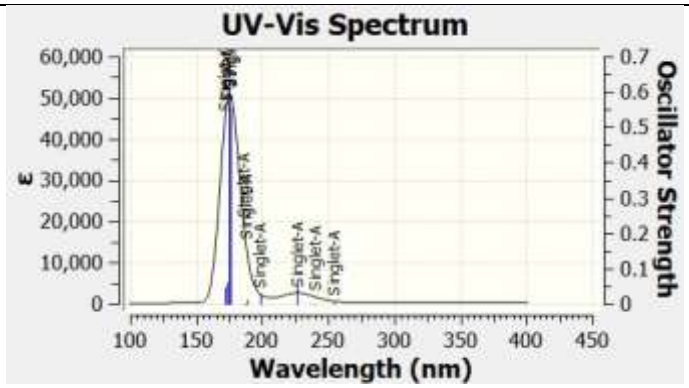

(a)

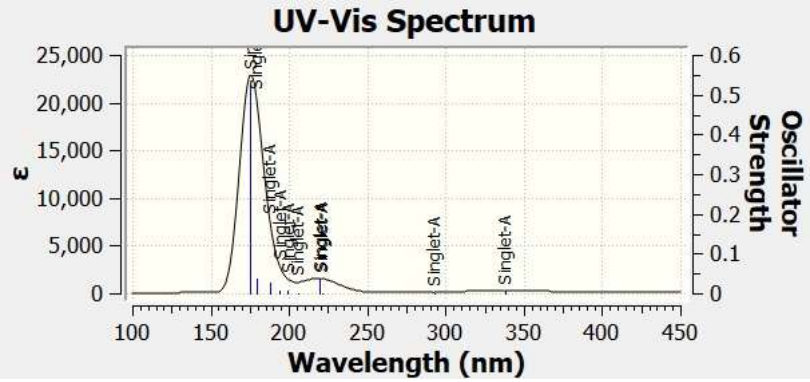

(b)

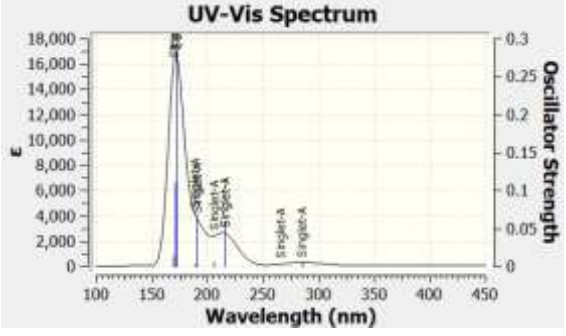

(c)

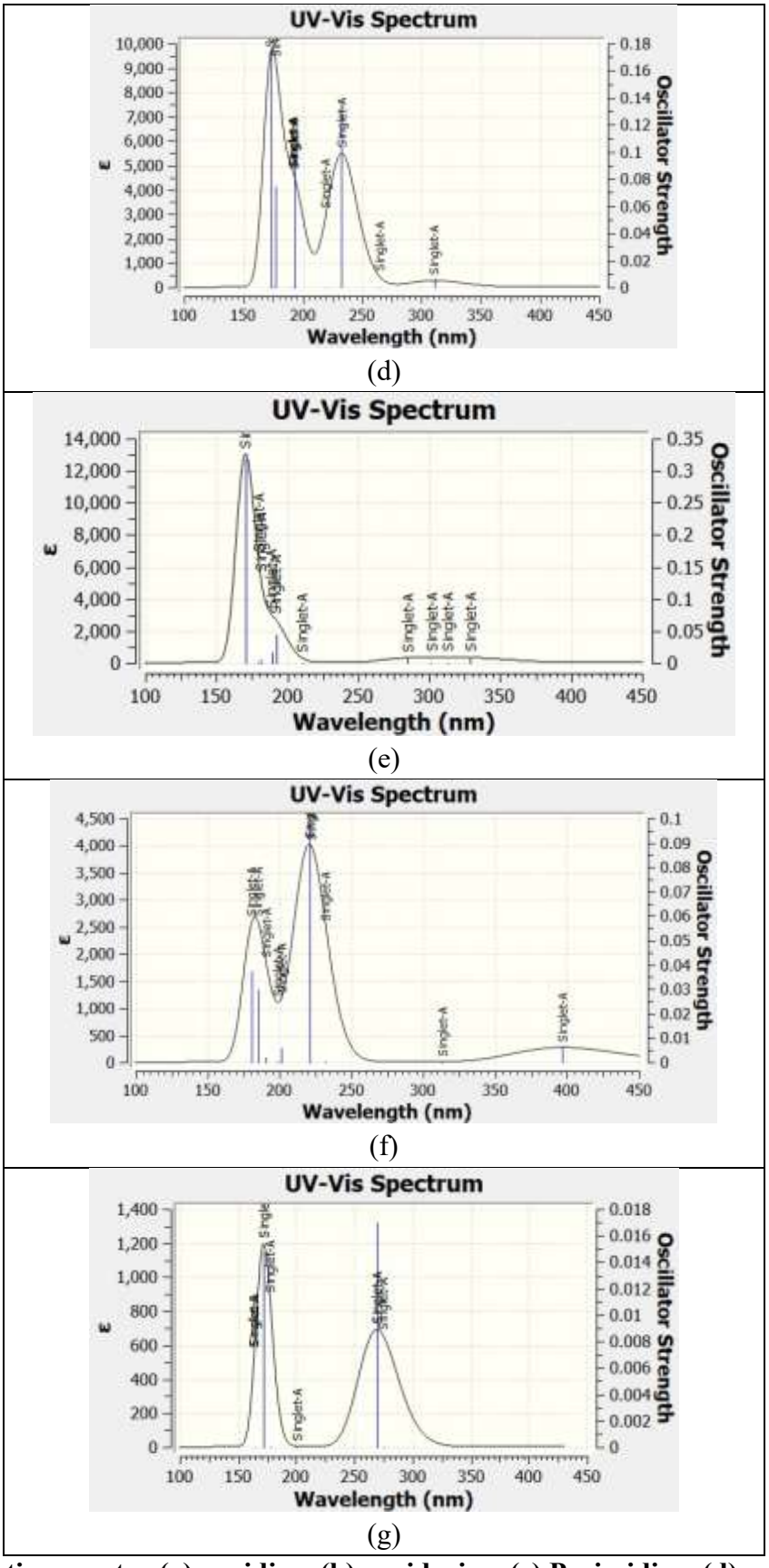

Figure 7: Absorption spectra (a) pyridine, (b) pyridazine, (c) Pyrimidine, (d) pyrazine, (e) 1,2,3-triazine, (f) 1,2,4-triazine and (g) 1,3,5-triazine in cyclohexane

Table 6. Excitation energies, corresponding wavelength, predominant transitions, and orbital contribution in cyclohexane

Systems	λ_{max}	f (oscillator frequency)	Orbital contribution	FMO	Energy (eV)
Pyridine	176.0 226.6	0.58 0.05	0.53 0.67	HOMO-2→LUMO+1 HOMO-1→LUMO	7.06 5.47
Pyridazine	175.3 219.8	0.59 0.04	0.53 0.61	HOMO-1→LUMO+1 HOMO-1→LUMO	7.07 5.63
Pyrimidine	172.0 216.1	0.30 0.06	0.58 0.62	HOMO→LUMO+4 HOMO-1→LUMO	7.20 5.73
Pyrazine	172.7 232.8	0.17 0.13	0.63 0.67	HOMO+1→LUMO+5 HOMO-1→LUMO	7.18 5.31
1,2,3-triazine	170.4 191.9	0.32 0.04	0.44 0.58	HOMO-2→LUMO+1 HOMO-2→LUMO	7.27 6.46
1,2,4-triazine	180.7 220.9 396.6	0.03 0.09 0.01	0.70 0.66 0.71	HOMO→LUMO+3 HOMO-1→LUMO HOMO→LUMO	6.86 5.61 3.12
1,3,5-triazine	172.1 269.4	0.01 0.02	0.70 0.52	HOMO-1→LUMO+2 HOMO→LUMO+1	7.20 4.6

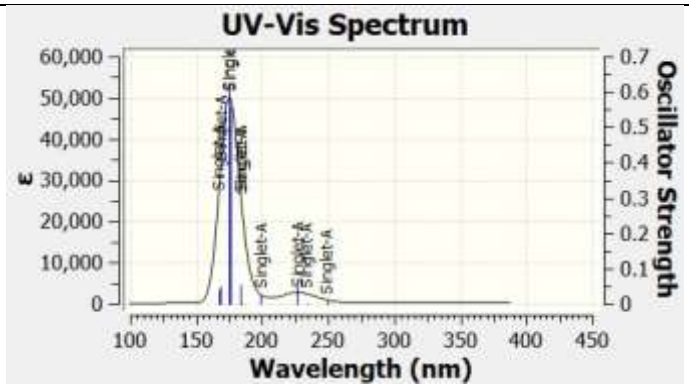

(a)

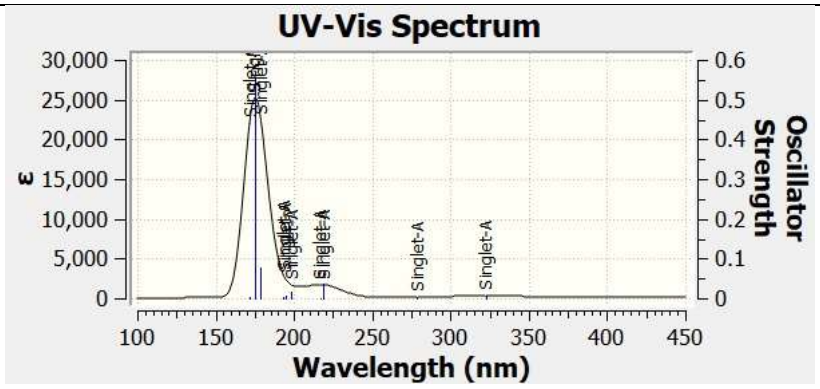

(b)

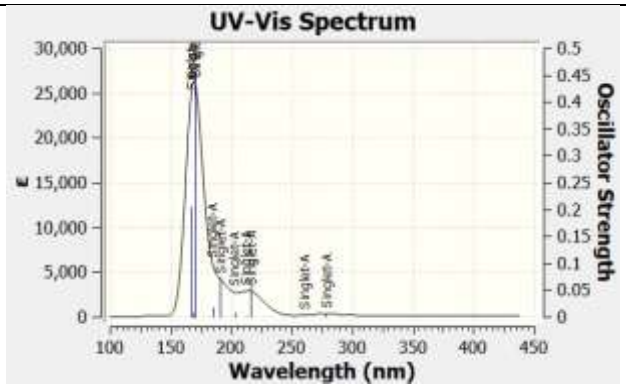
UV-Vis Spectrum
ε
Oscillator Strength
Wavelength (nm)
Singlet-A

(c)

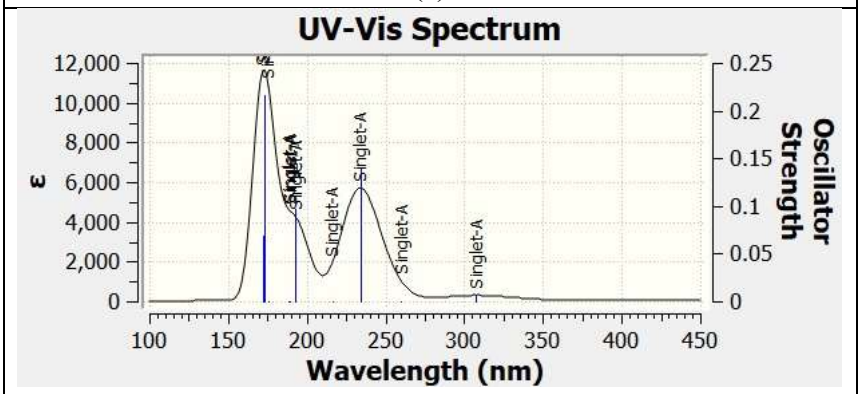
UV-Vis Spectrum
ε
Oscillator Strength
Wavelength (nm)
Singlet-A

(d)

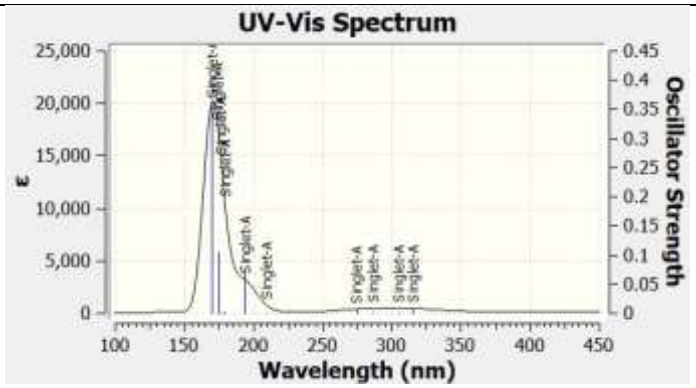
UV-Vis Spectrum
ε
Oscillator Strength
Wavelength (nm)
Singlet-A

(e)

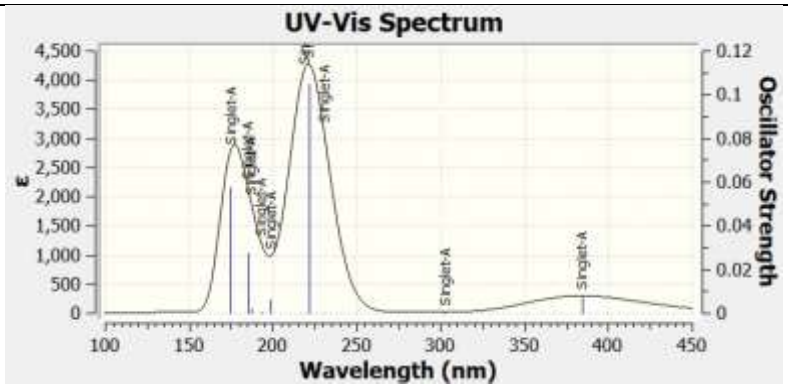
UV-Vis Spectrum
ε
Oscillator Strength
Wavelength (nm)
Singlet-A

(f)

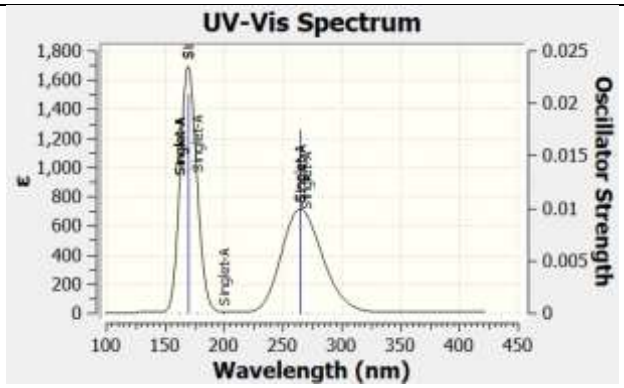

(g)

Figure 8: Absorption spectra (a) pyridine, (b) pyridazine, (c) Pyrimidine, (d) pyrazine, (e) 1,2,3-triazine, (f) 1,2,4-triazine and (g) 1,3,5-triazine in DMSO

Table 7. Excitation energies, corresponding wavelength, predominant transition and orbital contribution in DMSO

Systems	λ_{max}	f (oscillator frequency)	Orbital contribution	FMO	Energy (eV)
Pyridine	175.3 226.5	0.61 0.06	0.51 0.62	HOMO-2→LUMO HOMO-1→LUMO	7.07 5.47
Pyridazine	175.3 219.7	0.52 0.04	0.52 0.60	HOMO-1→LUMO+1 HOMO-1→LUMO	7.07 5.64
Pyrimidine	170.4 216.2	0.45 0.06	0.48 0.62	HOMO-2→LUMO HOMO-1→LUMO	7.27 5.73
Pyrazine	172.0 192.8 234.0	0.07 0.10 0.14	0.70 0.64 0.67	HOMO+1→LUMO+3 HOMO-1→LUMO+1 HOMO-1→LUMO	7.20 6.43 5.30
1,2,3-triazine	170.0 194.0	0.41 0.07	0.46 0.63	HOMO-2→LUMO+1 HOMO-2→LUMO	7.29 6.39
1,2,4-triazine	174.8 221.4	0.06 0.10	0.70 0.66	HOMO→LUMO+3 HOMO-1→LUMO	7.09 5.60
1,3,5-triazine	169.8 265.0	0.02 0.02	0.70 0.51	HOMO-1→LUMO+2 HOMO→LUMO+1	7.30 4.68

4. Conclusion:

In this study, an effort is made to understand the global reactivity of the concerned N-heterocyclic systems in the light of DFT. It is seen the global reactivity changes with the change in the number and positions on N-atom in the heterocycles. This is expected to prove handy for synthetic chemist and boost experimental works on these heterocycles. Aromaticity of these heterocycles varies with the number and positions on N-atom in the heterocycles. At around 1.0 Å from the molecular plane maximum aromaticity is observed, indicating maximum π-contribution at this distance. Presence of solvent phase has some impact on the reactivity of the considered 6 membered N-heterocycles. However, aromaticity is independent of presence of solvent phase. UV-Visible absorption spectra are predominantly within the UV region with slight red shift in presence of solvents.

References:

1. B. Eftekhari-Sis, M. Zirak, A. Akbari, Arylglyoxals in synthesis of heterocyclic compounds, *Chem. Rev.* 113 (2013) 2958–3043, https://doi.org/10.1021/cr300176g
2. K. S. Rajini, P. Aparna, C. Sasikala, C. V. Ramana, Microbial metabolism of pyrazines, *Crit. Rev. Microbiol.* 37 (2011) 99–112, https://doi.org/10.3109/1040841X.2010.512267
3. S. B. Ferreira, C. R. Kaiser, Pyrazine derivatives: a patent review – present, *Expert Opin. Ther. Pat.* 22 (2012) 1033–1051, https://doi.org/10.1517/13543776.2012.714370
4. S. S. Arunkumar, A review on synthetic heterocyclic compounds in agricultural and other applications, *Int. J. Pharm.Tech. Res.* 8 (2015) 170–179, https://doi.org/10.5958/0976-5506.2018.01544.9.
5. L. A. Mitscher, Bacterial topoisomerase inhibitors: quinolone and pyridone antibacterial agents, *Chem. Rev.* 105 (2005), 105, 559-592, https://doi.org/10.1021/cr030101q
6. L. E. Seitz, W. J. Suling, R. C. Reynolds, Synthesis and antimycobacterial activity of pyrazine and quinoxaline derivatives, *J. Med. Chem.*, 45 (2002), 5604-5606 https://doi.org/10.1021/jm020310n
7. I. Nenner, G. J. Schulz, Temporary negative ions and electron affinities of benzene and *N* heterocyclic molecules: pyridine, pyridazine, pyrimidine, pyrazine, and *s*-triazine *J. Chem. Phys.,* 1975 62 1747–1758, https://doi.org/10.1063/1.430700
8. M. Berthelot, C. Laurence, M. Safar, F. Besseau, Hydrogen-bond basicity pK HB scale of six-membered aromatic N-heterocycles, *J. Chem. Soc., Perkin Trans. 2, 1998,* 283-290, https://doi.org/10.1039/A706696A
9. R. G. Parr, R. G. Pearson, Absolute hardness: companion parameter to absolute electronegativity *J. Am. Chem. Soc.* 1983 105 7512-7516 https://doi.org/10.1021/ja00364a005
10. R. G. Parr, R. A. Donnelly, M. Levy, W. E. Palke, Electronegativity: the density functional viewpoint, *J. Chem. Phys.* 1978 68 3801-3807 https://doi.org/10.1063/1.436185
11. T. A. Koopmans, Über die Zuordnung von Wellenfunktionen und Eigenwerten zu den einzelnen Elektronen eines Atoms, *Physica,* 1933 1 104-113 https://doi.org/10.1016/S0031-8914(34)90011-2
12. R. G. Parr, L. V. Szentpaly, S. Liu, Electrophilicity Index, *J. Am. Chem. Soc.* 1999 121 1922-1924, https://doi.org/10.1021/ja983494x
13. M. J. Frisch et al. *Gaussian 09*, Gaussian, Inc., Wallingford CT, 2010
14. Z. Chen, C. S. Wannere, C. Corminboeuf, R. Puchta and P. v. R. Schleyer, Nucleus-independent **chemical** shifts (NICS) as an aromaticity criterion, *Chem. Rev.,* 2005 105 3842-3888, https://doi.org/10.1021/cr030088+
15. D. Jacquemin, E. A. Perpete, G. E. Scuseria, I. Ciofini and C. Adamo, TD-DFT Performance for the Visible Absorption Spectra of Organic Dyes: Conventional versus Long-Range Hybrids, *J. Chem. Theory Comput.* 2008, 4 123-135, https://doi.org/10.1021/ct700187z
16. J. Tomasi, B. Mennucci and R. Cammi, Quantum mechanical continuum solvation models *Chem. Rev.*, 2005, 105, 2999-3094, https://doi.org/10.1021/cr9904009
17. C. H. Suresh, G. S. Remya, P. K. Anjalikrishna, **Molecular** electrostatic potential analysis: A powerful tool to interpret and predict chemical reactivity *WIREs Comput. Mol. Sci.*, 2022, 12, e1601, https://doi.org/10.1002/wcms.1601
18. B. Saha and P. K. Bhattacharyya, Understanding reactivity, aromaticity and absorption spectra of carbon cluster mimic to graphene: a DFT study *RSC Adv.,* 2016 6 79768–79780, https://doi.org/10.1039/C6RA15016K

19. T. M. Krygowski, H. Szatylowicz, O. A. Stasyuk, J. Dominikowska and M. Palusiak, Aromaticity from the viewpoint of molecular geometry: application to planar systems, *Chem. Rev.*, 2014 114 6383-6422, https://doi.org/10.1021/cr400252h
20. C. Corminboeuf, T. Heine, G. Seifert, P. von Ragué Schleyer and J. Weber, Induced magnetic fields in aromatic [n]-annulenes-interpretation of NICS tensor components, *Phys. Chem. Chem. Phys.*, 2004, 6, 273-276, https://doi.org/10.1039/B313383B
21. A. Stanger, Nucleus-independent chemical shifts (NICS): distance dependence and revised criteria for aromaticity and antiaromaticity, *J. Org. Chem.* 2006 71 883-893, https://doi.org/10.1021/jo051746o
22. M. J. Peach, P. Benfield, T. Helgaker and D. J. Tozer, Excitation energies in density functional theory: An evaluation and a diagnostic test *J. Chem. Phys*, 2008, 128, 044118, https://doi.org/10.1063/1.2831900
23. E. B. Hughes, H. H. G. Jellinek, B. A. Ambrose, Pyridine. Ultraviolet Absorption Spectrum and Dissociation Constant, *J. Phys. Chem.* 1949, 53, 3, 410–414, https://doi.org/10.1021/j150468a009
24. B. Samira, C. Kalaliana, E. Rotha, R. Salghib, A. Chakira, Gas-phase UV absorption spectra of pyrazine, pyrimidine and pyridazine, *Chem. Phys. Lett.* 2020 751 137469, https://doi.org/10.1016/j.cplett.2020.137469